Impact of Proximity Effect on Uranyl Coordination of Conformationally Variable Weakly-Bonded Cucurbit[6]uril-Bipyridinium Pseudorotaxane

Feize Li,[a, b] Lei Mei,[b] Haiyue Peng,[a] Kongqiu Hu,[b] Zhifang Chai,[b, c] and Ning Liu*[a]*

[a] Key Laboratory of Radiation Physics and Technology of the Ministry of Education, Institute of Nuclear Science and Technology, Sichuan University, Chengdu 610064, P. R. China.

[b] Laboratory of Nuclear Energy Chemistry, Institute of High Energy Physics, Chinese Academy of Sciences, Beijing 100049, P. R. China.

[c] Engineering Laboratory of Advanced Energy Materials, Ningbo Institute of Industrial Technology, Chinese Academy of Sciences, Ningbo, Zhejiang, 315201, P. R. China.

Corresponding Author

*E-mail: meil@ihep.ac.cn (Mei Lei); nliu720@scu.edu.cn (Ning Liu)

Abstract. To explore the proximity effect in uranyl coordination of weak-bonded cucurbit[6]uril(CB[6])-bipyridinium ligands, a new pseudorotaxane precursor **C7BPCN3**@CB[6] containing 1, 1'-(heptyl-1,7-diyl)bis(3-cyanopyridin-1-ium) bromide (**C7BPCN3**) with elongated alkyl chains and *meta*-substituted cyano groups, has been synthesized and used to react with the uranyl cations. Due to the weak binding affinity between the host and guest components of the supramolecular ligand, five new uranyl-rotaxane coordination polymers **URCP1-URCP5** have been prepared, in which the pseudorotaxane linkers have shown great conformation diversity and abundant coordination behaviors. Three different coordination modes are present in these as-synthesized uranyl compounds, one of which is host-guest synergetic coordination due to the proximity effect between the *meta*-coordination carboxylate groups of **C7BPCN3** and the portal carbonyls of CB[6]. Specially, the elongated spacer and weak-bonded feature make only one end of **C7BPCN3**@CB[6] ligand involved in host-guest synergetic chelating with the uranyl centre, leaving the other one participated in metal-organic coordination only by the guest. It is the first time that this unique coordination mode has been observed in uranyl coordination polyrotaxanes. This work demonstrates the proximity effect on uranyl coordination of weak-bonded CB[6]-bipyridinium pseudorotaxane linkers, and provide an alternative approach to achieve metal coordination regulation and structure diversity in uranyl coordination polymers involving mechanically interlocked molecules.

Introduction

Recently, uranium-organic materials (UOMs) featured with uranyl cations/clusters acting as metal nodes have drawn more and more attention[1-2]. After exquisite designs, abundant UOMs varying from zero-dimensional (0D) to three-dimensional (3D) have been synthesized[3-4], which have dramatically facilitated the recognition of actinide chemistry, especially those involving solid-state coordination polymers. On the other hand, benefitting from the special characteristics of the actinide elements, new uranyl-based functional materials with potential application in high-performance separation[5-9], selective detection[10-11], chemical sensing,[12-13] and heterogeneous catalysis[14-16] have been also reported. Although the development of functional UOMs has made great progresses in the past decade, it's still at the early stage when compared with the well-studied metal-organic materials based on transition metal elements. Hence, the design and synthesis of new UOMs is still of great significance in solid-state chemistry of actinides.

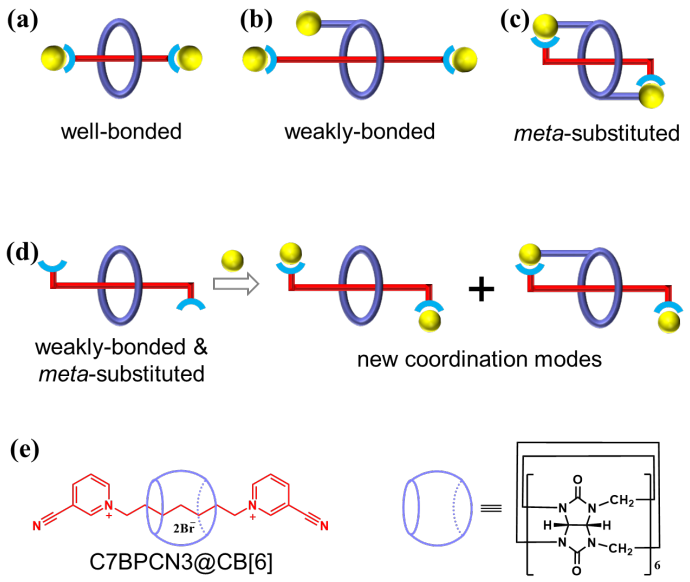

Scheme 1. (a) The most common connecting pattern of well-bonded pseudorotaxane ligand: only the string guest with end functional groups coordinates with the uranyl centre. (b) Weakly-bonded pseudorotaxane ligand can produce a new connecting pattern: both the CB[6] host and the string guest can simultaneously coordinate with different uranyl centre. (c) For the pseudorotaxane ligand with meta-substituted carboxylate groups: both the host and guest components can synergistically coordinate with the same uranyl centre. (d) New coordination modes may be expected in the weakly-bonded pseudorotaxane with meta-substiteted functional groups. (e) The presentation of the weakly-bonded **C7BPCN3**@CB[6] ligand with the functional groups located at meta-position.

Due to the restrained first coordination sphere of uranyl caused by the intrinsic axial oxygen atoms, introducing new ligands might be a highly feasible way to obtain novel UOMs with novel

structures and special features. Among all the available organic linkers, pseudorotaxanes have been demonstrated to be a kind of versatile precursors which can endow the prepared materials with unique topologies[17-18] and molecular dynamics[19-21]. In a typical pseudorotaxane, the macrocyclic host and the string guest bond with each other through weak interactions between these two components. This provides an important platform for designing new organic ligands through non-covalent binding, which can produce richer variations in the linkers than direct chemical modification. In addition, pseudorotaxanes can exhibit plenty of coordination behaviors during the assembly with metal cations, since the intermolecular interactions may lead to much more flexibility in the supramolecular linkers.

However, for most pseudorotaxanes, especially these based on CB[6], an inevitable issue is that the macrocyclic hosts in well-bonded precursors were not easy to participate in the coordination with the metal centres[22-27]. Usually, only the di-cationic guest flanked with two chelate ligands can coordinate with the uranyl centre, with the macrocyclic host hanging on the skeleton (Scheme 1a). To address such problem, we proposed two approaches in the previous work concerning CB[6]-based uranyl-rotaxane coordination polymers (URCPs). The first one is applying weakly-bonded host-guest complexes as precursors to react with uranyl cations.[28-30] For instance, when the alkyl chain was prolonged from hexyl (C6) to heptyl (C7), the guests size would not well match the cavity of the CB[6] host, which could effectively reduce the steric hindrance around the portal carbonyl groups. Therefore, the CB[6] hosts could simultaneously approach the metal cations like the string molecules, but coordinate with different uranyl centres (Scheme 1b).

Another regulation strategy was moving the end carboxylate groups from *para*- to *meta*-position[31]. This strategy has also been demonstrated to be effective, even for the well-bonded CB[6]-based pseudorotaxane ligand (*i.e.* those with the guest length being as C6), since the special molecular configuration could produce proximity effect around the portals, resulting in a host-guest synergetic coordination mode (both the macrocyclic host and the string guest coordinate with the same uranyl centre) in related uranyl polyrotaxanes (Scheme 1c). Based on the foregoing research, an interesting question is what effect will the combination of the above two strategies have on the assembly of uranyl rotaxane coordination compounds. Obviously, this may result in a more complicated effect on the coordination mode of pseudorotaxane, such as a mixture of multiple behaviors in one compound including unilaterally-synergetic coordination mode (Scheme 1d).

In this work, with an attempt to investigate the possible new coordination modes of weakly-bonded pseudorotaxane with meta-substituted functional groups in URCPs, we pre-assembled 1,1'-(heptyl-1,7-diyl)bis(3-cyanopyridin-1-ium) bromide (**C7BPCN3**) and CB[6] to give a weakly-bonded pseudorotaxane precursor (**C7BPCN3**@CB[6]) with the end functional groups located at the *meta*-position (Scheme 1e). Then this new pseudorotaxane was used to react with uranyl cations, leading to five uranyl coordination polyrotaxanes **URCP1-URCP5** with 1D or 2D structures. The connecting patterns of the pseudorotaxane ligands have been demonstrated to show abundant variety, and the structure-dependent regulation mechanism of these URCPs is discussed in detail. The physico-chemical properties of these prepared URCPs have also been characterized by thermogravimetric analysis, infrared spectroscopy, and photoluminescent spectroscopy.

Methods and Experiments.

Table S1. The synthetic information for **URCP1-URCP5**.

	URCP1	**URCP2**	**URCP3**	**URCP4**	**URCP5**
C7BPCN3@CB[6] (mg)	30.0	30.0	30.0	30.0	30.0
0.5 M $UO_2(NO_3)_2$ (μL)	70	70	70	70	70
$Na_2C_2O_4$ (mg)	0	4.5	0	0	0
Na_2SO_4 (mg)	0	0	5.0	5.0	5.0
H_2O (mL)	2	2	2	2	2
4 M HNO_3 (μL)	0	10	10	0	0
1 M NaOH (μL)	0	0	0	0	20
temp (°C)	150	150	150	150	150
time (h)	72	72	72	72	72
yield (%) based on uranium	40.5	—	—	78.2	62.4

For the syntheses of **URCP1** ($(UO_2)_2(\mu_2\text{-}OH)_2Br(NO_3)$(**C7BPCA3**@CB[6])$_2\cdot 2H_2O$), **URCP2** ($(UO_2)_2(C_2O_4)(NO_3)_2$(**C7BPCA3**@CB[6])$\cdot 4H_2O$), **URCP3** ($(UO_2)_2(SO_4)_2(H_2O)_4$(**C7BPCA3**@CB[6])$\cdot 8H_2O$), **URCP4** ([$(UO_2)(H_2O)_3$(**C7BPCA3**@CB[6])$_4\cdot$($(UO_2)_2(SO_4)_2(\mu_2\text{-}OH)_2$(**C7BPCA3**@CB[6])$_4$]HCl)) and **URCP5** ($(UO_2)_3(SO_4)_2(H_2O)(\mu_2\text{-}OH)_2$(**C7BPCA3**@CB[6])$_2\cdot 6H_2O$), 30.0 mg of pseudorotaxane

precursor **C7BPCN3**@CB[6] and 70 μL of uranyl nitrate (0.5 M) were added into a Teflon lined stainless-steel vessel. After adding 2 mL of deionized water, the reactors were transferred into an oven and heated at 150 ºC for 72 h. After naturally cooling to room temperature, yellow single crystals were collected from the solution for single crystal X-ray diffraction. The remained were alternatively rinsed with water and ethanol for 3~5 times, and dried at 50 ºC overnight for further characterizations. Additionally, two small co-existing anions (oxalate and sulfate) with different coordination capacity were also introduced into the reaction system, in order to regulate the coordination behaviors of the pseudorotaxane ligands and the final structure of obtained compounds. The synthetic conditions are listed in Table 1.

The single crystal X-ray diffractions for all obtained compounds were performed on Bruker D8 VENTURE X-ray CMOS diffractometer with a Mo Kα (λ = 0.71073 Å) or a Cu Kα (λ = 1.54184 Å) X-ray source at room temperature or 170 K according to the crystal qualities.. The powder X-ray diffraction (PXRD) spectra were performed on a Bruker D8 Advance diffractometer with Cu Kα radiation (λ = 1.5406 Å). The thermogravimetric analyses (TGA) were determined on a TA Q500 analyzer. A Bruker Invenio-R spectrometer was employed to obtain the Fourier transform infrared (FTIR) spectra. Solid-state photoluminescence (PL) spectra were obtained using a Hitachi F-4600 fluorescence spectrophotometer. ^{1}H-NMR spectra were recorded on a Bruker AVANCE III (500 MHz, Bruker, Switzerland) with deuterium oxide as a solvent. ESI-MS spectra were obtained with a Bruker AmaZon SLion-trap mass spectrometer (Bruker, USA).

For **C7BPCA3**@CB[6] and **URCP1-URCP5**, the single crystal X-ray diffractions data were integrated with the SAINT software package, and multi-scan absorption correction was completed using SADABS. The crystal structures for all compounds were solved by means of direct methods (SHELXL-97[32]) and refined with full-matrix least squares techniques on F^2 using SHELXL-2018[32-33] and *Olex*2[34] software packages. Hydrogen atoms of the carbon atoms and water molecules were added at theoretically calculated positions, treated as riding ones with isotropic displacement parameters 1.2 times higher than that of the parent atoms. Due to the disordered structures, some hydrogen atoms originally belonging to part of the water solvent molecules in **URCP2**, **URCP3** and **URCP5** could not be added. For **URCP5**, PLATON/SQUEEZE[35] was applied to calculate the diffraction contribution of the solvent molecules and further refinements were performed based on the obtained new sets of diffraction intensity. The coordinated bromide anion was split into three parts, because of the disordered structure. Other restraints such as ISOR and DFIX have also been

adopted in the uranyl coordination polymers, to achieve better refinements. Crystal data of all compounds are listed in Table 2, and the selected bond lengths are listed in Table S1. Crystallographic data in this work have been deposited with Cambridge Crystallographic Data Centre, and the CCDC numbers are: 2105868 (**C7BPCA3**@CB[6]), 2105869 (**URCP1**), 2105870 (**URCP2**), 2105871 (**URCP3**), 2105872 (**URCP4**) and 2105873 (**URCP5**).

Table 2. Crystallographic data and structure refinement results for **C7BPCA3**@CB[6] and **URCP1**-**URCP5**.

	C7BPCA3@CB[6]	**URCP1**	**URCP2**
formula	$C_{55}H_{90}N_{26}O_{32}$	$C_{110}H_{120}BrN_{54}O_{60}U_4$	$C_{57}H_{59}N_{28}O_{34}U_2$
fw	1627.52	4190.62	2159.40
crystal sys	monoclinic	monoclinic	triclinic
space group	*C*2/c	*C*c	$P\bar{1}$
***a*, Å**	15.0060(13)	18.3214(7)	12.304(2)
***b*, Å**	20.6811(16)	17.8962(7)	12.4966(18)
***c*, Å**	22.944(2)	22.4009(9)	13.125(2)
***α*, degree**	90	90	64.880(6)
***β*, degree**	99.494(4)	113.982(3)	89.809(6)
***γ*, degree**	90	90	79.159(6)
***V*, Å^3**	7022.8(10)	6710.8(5)	1787.8(5)
***T*, K**	293	292	292
***F* (000)**	3432.0	4052.2	1042.0
***D*c (g cm^{-3})**	1.539	2.064	1.987
***μ* (mm^{-1})**	0.127	5.097	4.639
R_{int}	0.0512	0.0524	0.0782
***R*1, *wR*2**	0.0556, 0.1561	0.0270, 0.0626	0.0423, 0.1035
	URCP3	**URCP4**	**URCP5**
formula	$C_{55}H_{82}N_{26}O_{40}S_2U_2$	$C_{110}H_{122}ClN_{52}O_{51}S_2U_3$	$C_{110}H_{128}N_{52}O_{56}S_2U_3$
fw	2287.61	3802.25	3852.85
crystal sys	triclinic	orthorhombic	monoclinic
space group	$P\bar{1}$	$P2_12_12_1$	$P2_1$/c
***a*, Å**	12.4914(7)	23.1168(13)	23.0996(13)
***b*, Å**	13.5836(7)	24.6194(15)	18.4319(11)
***c*, Å**	13.6906(6)	24.9596(10)	33.9541(19)
***α*, degree**	105.650(2)	90	90
***β*, degree**	95.320(2)	90	103.095(2)
***γ*, degree**	113.732(2)	90	90
***V*, Å^3**	1993.62(18)	14205.1(13)	14080.7(14)
***T*, K**	292	302	143
***F* (000)**	1111.0	7516.0	7632.0
***D*c (g cm^{-3})**	1.885	1.778	1.817
***μ* (mm^{-1})**	4.220	3.567	10.850
R_{int}	0.051	0.1397	0.0631

***R*1, *wR*2**	0.0506, 0.1496	0.0881, 0.2746	0.0439, 0.1159

Structure Description. URCP1crystallizes in the space group of *C*c and is a chain-like compound. The uranyl centre is dimeric and both uranium atoms are 7-fold coordinated (Figure 1a and S5). For U1, besides the two axial oxygen atoms, there are two oxygen atoms from a bidentate carboxylate group of **C7BPCA3**, two μ_2-hydroxyl oxygen atoms and a bromide anion coordinating with the metal centre from the equatorially plane. U2 centre, the other uranium unit of dimeric uranyl node, has a slightly different coordination sphere. Except two axial oxygen atoms and two shared μ_2-oxo oxygen atoms, two oxygen atoms from a bidentate-coordinated nitrate anion and one oxygen atom from the carboxylate group of **C7BPCA3** coordinate with U2. The U=O distances vary from 1.768(9) to 1.777(1) Å, with the angles of O=U=O being 179.4(4)° (U1) and 175.8(5)° (U2). The U-O bond lengths range from 2.273(11) to 2.529(10) Å. Specifically, the U-Br is found to be 2.805(5) Å, which is quite consist with the previous work.[31] **C7BPCA3** linkers connect the dimeric uranyl nodes to form a zigzag chain (Figure 3b), with the CB[6] hosts hanging on the chain like beads.

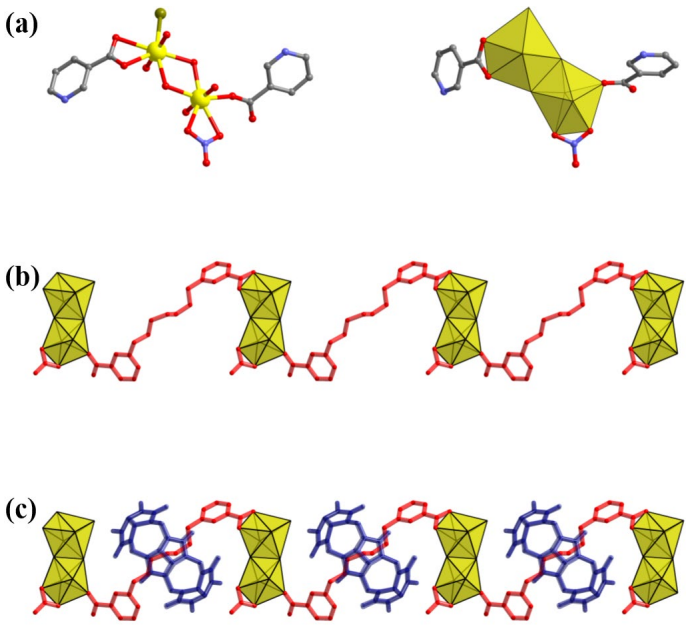

Figure 1. (a) Coordination environment for the dimeric uranyl centre in **URCP1**: the left is the one with the uranyl centre is shown as stick-ball mode and the right is shown as polyhedron mode. (b) The 1D uranyl-directed chain linked by **C7BPCA3** guests (c) The CB[6] hosts hang on the alkyl chains of **C7BPCA3** guests.

URCP2 is a chain-like polyrotaxane that crystallizes in the space group of $P\bar{1}$. As shown in Figure 2a and S6, a dimeric metal node bridged by an oxalate anion can be observed in this compound, of

which two uranium centres are both 8-fold coordinated and crystallographically equivalent with each other. In addition to the two intrinsic axial oxygen atoms of uranyl cation, there are other six ones in the equatorial plane. Specifically, a bidentate-coordinated carboxylate group from **C7BPCA**3, a bidentate-coordinated nitrate anion together with a bilaterally-chelated oxalate anion has bound to the uranyl cation, respectively. The U=O bond lengths are 1.736(8) and 1.737(8) Å, while the O=U=O angle is measured to be 179.0(4)°. The U-O bond lengths is found to be in the range of 2.434(7) ~ 2.561(8) Å. The uranyl dimers are connected by **C7BPCA** linkers, forming an 1D chain with nitrate anions located at the terminals (Figure 2b). CB[6] hosts, like the macrocyclic molecules presented in most cases involving cucurbituril-based uranium coordination polymers, just hang on the skeleton of the chain-like compounds, without coordination with the metal centres (Figure 2c).

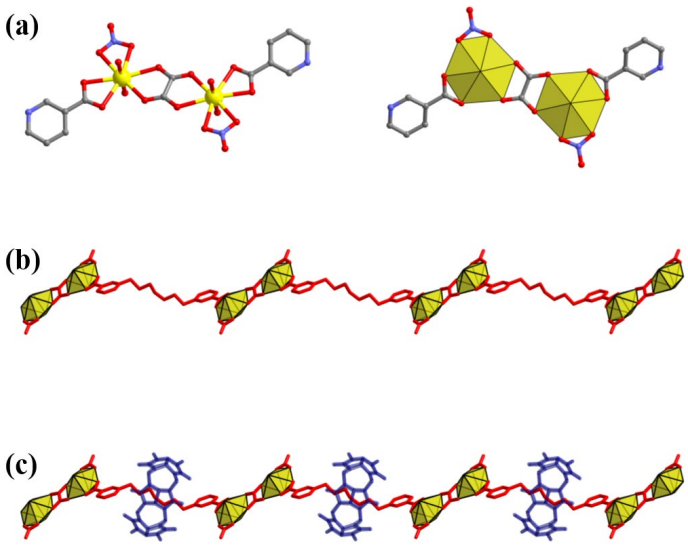

Figure 2. (a) Coordination environment for the dimeric uranyl centre in **URCP2**: the left is one with the uranyl centre is shown as stick-ball mode and the right is shown as polyhedron mode. (b) The 1D uranyl-directed chain linked by **C7BPCA3** guests, with oxalate and nitrate anions locate at the terminal of the metal cations. (c) The CB[6] hosts hang on the alkyl chains of **C7BPCA3** guests.

URCP3 is also a 1D chain-like compound and crystallizes in the space group of $P\bar{1}$. As shown in Figure 3a and S7a, two sulfate anions bridge two uranyl cations to give a dimeric metal centre. The two uranium atoms are crystallographically equivalent and 7-fold coordinated. There are two axial oxygen atoms, one oxygen atom from a carboxylate group of **C7BPCA3**, two oxygen atoms from two sulfate anions and two water molecules in the coordination sphere of the uranium atom. The

O=U=O angle is found to be 178.0(3)°, while the U=O distance are 1.764(6) and 1.767(6) Å, respectively. For the oxygen atoms in the equatorial plane, U-O bond lengths vary from 2.311(6) to 2.483(6) Å. The sulfate-bridged uranyl nodes are further connected by **C7BPCA3**, resulting in a zigzag chain (Figure 3b). Different from **URCP1** and **URCP2**, both carboxylate groups at the terminals of the pyridinium rings are monodentate. CB[6] hosts prefer to interact with the metal nodes through O-H···O hydrogen bonds but not metal-ligand coordination (Figure 3c and S7b), with a H···O length of 2.015 Å. Besides, the coordinated water molecules can form intra molecular O-H···O bonds with the carboxylate oxygen atom, with the distances being 1.691 Å.

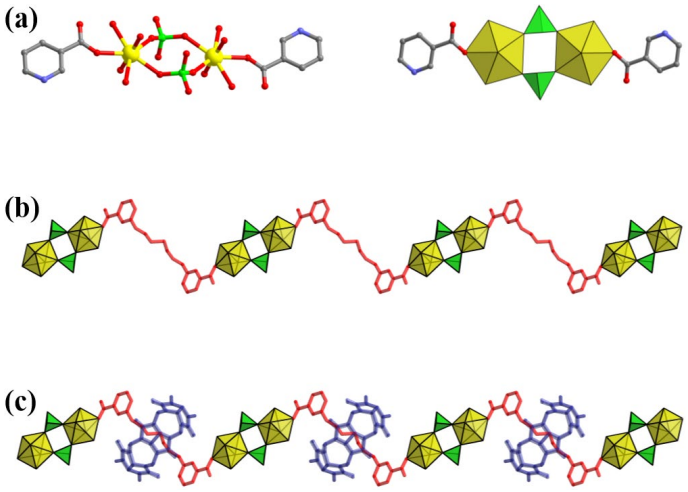

Figure 3. (a) Coordination environment for the dimeric uranyl centre in **URCP3**: the left is the one with the uranyl centre is shown as stick-ball mode and the right is shown as polyhedron mode. (b) The 1D uranyl-directed chain linked by **C7BPCA3** guests. (c) The CB[6] hosts hang on the alkyl chains of **C7BPCA3** guests.

URCP4 crystallizes in the space group of $P2_12_12_1$ and is a 1D chain-like polymers. Two types of uranyl centres can be observed in this compound, one is a monomeric uranyl centre and the other is a hydroxyl-bridged dimer, with all uranium atoms being 7-fold coordinated. For uranium atom in the mononuclear node, there are two axial oxygen atoms, two oxygen atoms from two carboxylates of **C7BPCA3** and three water molecules attending in the first coordination sphere (Figure 4a and S8a). Multiple O-H···O hydrogen bonds can be found between the coordinated water molecules and the host-guest complex (Figure S8b). The other uranyl centre in **URCP4** is dimeric and contains two uranium atoms with the same coordination environment, which are bridged by two hydroxyl anions (Figure 4b). For both uranium atoms, except the two axial oxygen atoms, one oxygen atom from the carboxylate group of **C7BPCA3**, two oxygen atoms from a bidentate-coordinated sulfate

anion and two μ_2-hydroxyl oxygen atoms are present in the equatorial plane. The U=O bond lengths are in the range of 1.77(5) ~ 1.84(2) Å, with the O=U=O angle varying from 176.1(11)° to 178.7(9)°. Meanwhile, the U-O distances in the equatorial planes of these three uranium atoms are in the range of 2.32(2) ~ 2.52(2) Å. As Figure 4c shows, two **C7BPCA3** molecules bond to both terminals of the sulfate-containing uranyl dimer through one end carboxylate groups, with the other ends further coordinating with another mononuclear uranyl nodes. A 1D kinked chain has formed, which is *N*-sharped when viewed from the side. All the CB[6] hosts just hang on the alkyl chain like that observed in **URCP1-URCP3**, without participating in the coordination with uranyl cations (Figure 4d).

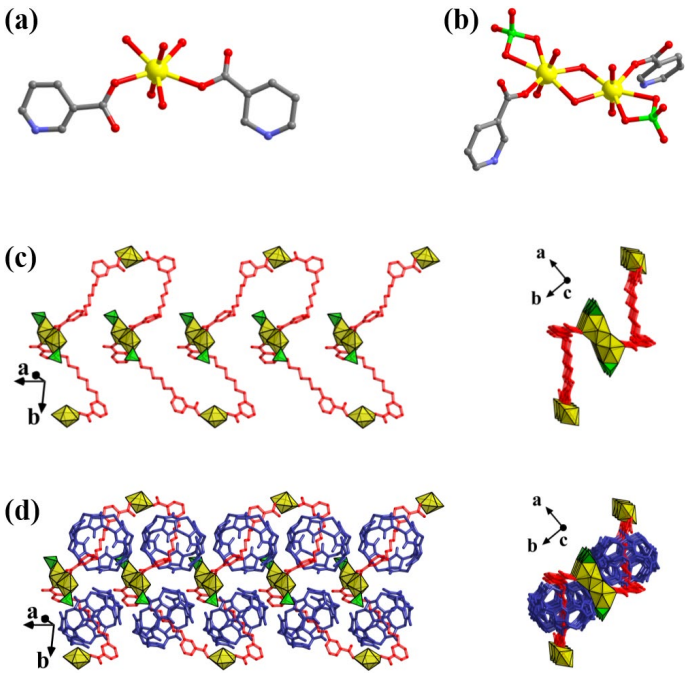

Figure 4. (a-b) Coordination environments for the two different uranyl centres in **URCP4.** (c) The 1D uranyl-directed chain linked by **C7BPCA3** guests, with two types of uranyl centres acting as nodes. (c) The CB[6] hosts hang on the alkyl chains of **C7BPCA3** guests.

URCP5 is a 2D compound crystallizing in the space group of $P2_1/c$. The metal node is a trimmer containing three 7-fold coordinated uranyl cations and two sulfate anions (Figure 5a and S9). For both U1 and U2, in addition to the two axial oxygen atoms, there are one oxygen atom from a carboxylate group of **C7BPCA3**, two oxygen atoms from a sulfate anion and two μ_2-hydroxyl oxygen atoms in the coordination sphere. For U3, there are two axial oxygen atoms, two oxygen atoms from two carboxylate groups of **C7BPCA3**, one oxygen atom from a sulfate anion, one

oxygen atom from a carbonyl group of CB[6] and a water molecule coordinating in the equatorial plane. The U=O bond lengths for all uranium atoms in the trimeric centre vary from 1.738(5) to 1.777(5) Å, with the O=U=O angle being in range of 176.7(2)° ~ 179.1(3)°. The U-O bond lengths in the equatorial planes of these three uranium atoms span from 2.257(6) to 2.530(5) Å. Specifically, CB[6] has also appeared in the coordination sphere of the uranyl centre (Figure 5b), which is quite similar to our previous work involving host-guest synergetic coordination of cucurbituril-based ligand in uranyl coordination polyrotaxane[31]. It seems that the uranyl dimers are first connected by the **C7BPCA3** molecules to form zigzag chains, with two sulfate anions located at the terminals of the uranyl nodes. Then, another array of pseudorotaxane ligands with a different orientation link different 1D chains one by one through a third monomeric uranyl anchored to the terminal sulfate ion, forming a special 2D network (Figure 5c and S10). Macrocyclic CB[6] hosts in **URCP5** present two types of behaviors. CB[6] host related to the zigzag chains just hang on the chain like beads (the blue ones shown in Figure 5d), while those in pseudorotaxane linkers for connecting 1D chains have coordinated to the uranyl cations together with the string **C7BPCA3** *via* a host-guest synergetic coordination mode (the pink ones shown in Figure 5d).

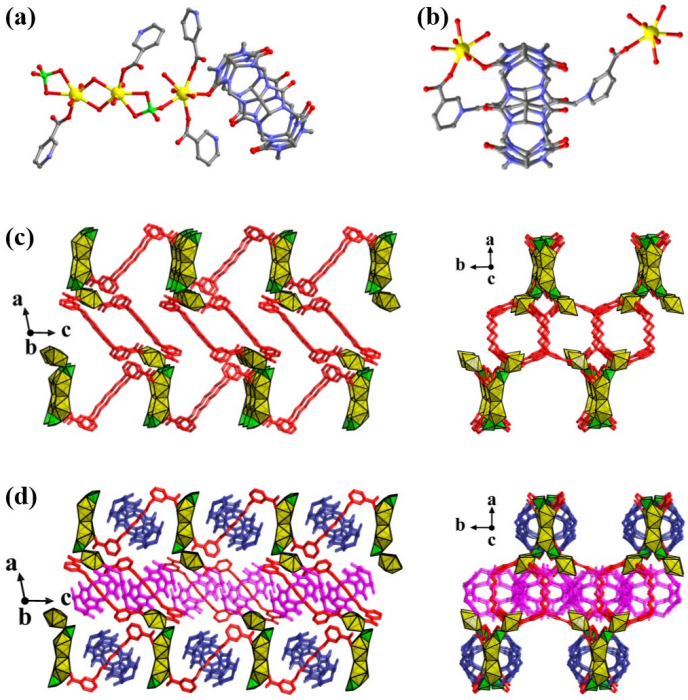

Figure 5. (a-b) Coordination environments for the two different uranyl centres in **URCP5.** (c) The 2D network linked by **C7BPCA3** guests, with two types of uranyl centres acting as nodes. (c) Two types of CB[6] observed in **URCP5**: the blue ones are those hanging on the skeleton without participating in the coordination with uranyl, and the pink are those synergistically coordinated with the uranyl centre together with **C7BPCA3** molecules.

Different Coordination Behaviors of C7BPCA3@CB[6] in Uranyl Coordination Polyrotaxanes. Actually, cucurbit[*n*]uril and their derivatives (CB[*n*], *n* = 5, 6, 7 and 8) have been demonstrated to be versatile struts, either as guest-free macrocyclic ligand or corresponding pseudorotaxanes, to build metal-organic coordination frameworks[36-38].The most obvious difference between the pure macrocyclic molecule and related supramolecular ligand is the coordination model. As for uranyl coordination complexes, when CB[*n*] molecules were used as organic linkers, they can mainly coordinate with metal cations through the portal carbonyl groups which have good affinity towards metal cations (Figure 6a)[39]. However, when CB[*n*] macrocycles were pre-assembled with string guests to give pseudorotaxane ligand, they prefer to be inert in the coordination with metal cations. As a result, only the guest molecules with functional ends (carboxylate groups) located at para or meta positions tend to bind with the uranyl center, either in monodentate- or bidentate-mode, while the macrocyclic hosts generally hang on the skeleton like beads (Figure 6b)[28-30]. Besides, if the end groups of the guests were cut off, uranyl might undergo no coordination with both component of the pseudorotaxane precursor, but only formed ionic cocrystal compound through the weak interaction such as hydrogen bonds between the pseudorotaxanes and metal center (Figure 6c)[21].

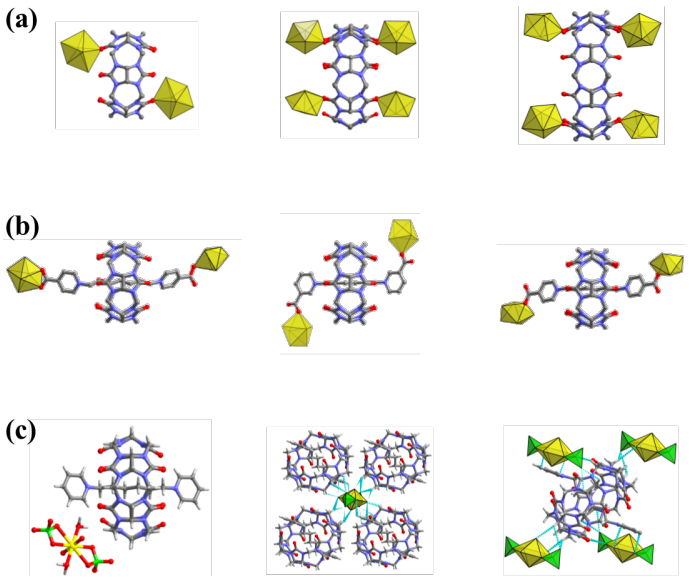

Figure 6. (a) Uranyl coordination compounds formed based on CB[6] (left), CB[7] (middle), and CB[8] (right)[39]. (b) General coordination mode or CB[6]-based pseudorotaxane in uranyl coordination polymers[28-30]. (c) Ionic cocrystal compound given by uranyl and CB[6]-pseudorotaxane without end functional group[21].

To achieve the simultaneous or synergetic metal-organic coordination of both components in

CB[*n*]-based pseudorotaxane ligand, we proposed to employ weakly-bonded host-guest complexes as organic linkers or introduce proximity effect into the well-defined pseudorotaxane ligand in previous work[28-31]. In the present work, we combined these two strategies into one precursor, *i.e.*, moving the functional groups of the guest molecule in a weakly-bonded ligand from the *para*- to *meta*-position. Due to the weak binding between the host and guest components, **C7BPCA3**@CB[6] motifs have shown different molecular conformations in **URCP1-URCP5**. As shown in shown in Figure 7, the configuration changes of the pseudorotaxane ligand can be well illustrated be variety of the distances between the two nitrogen cations of the pyridinium rings (*d*) and the angles between the CB[6] portal and the pyridinium ring (φ).

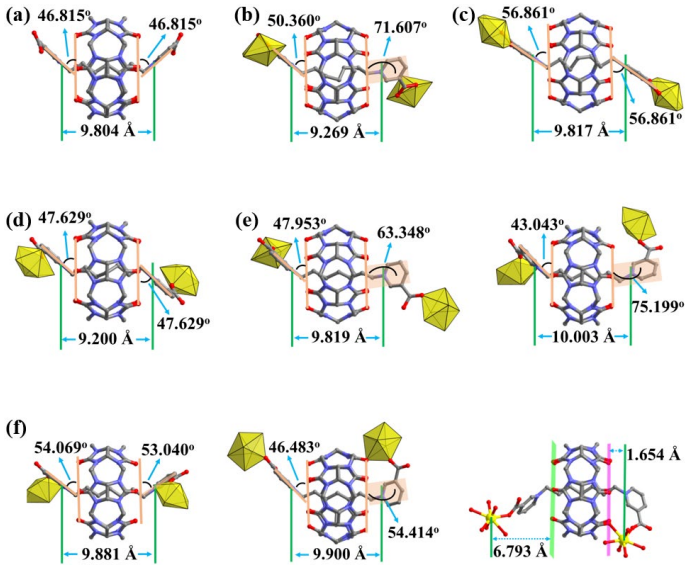

Figure 7. The values of *d* and φ in (a) metal-free **C7BPCA3**@CB[6] precursor, (b) **URCP1**, (c) **URCP2**, (d) **URCP3**, (e) **URCP4** and (f) **URCP5**.

Due to the rich molecular configuration of **C7BPCA3**@CB[6], three different coordination modes of the pseudorotaxane ligand can be found in the obtained URCPs (Figure 8a). Mode 1 is the most common and can be observed from **URCP1** to **URCP5** (Figure S11a). In this situation, only the dicarboxylate guest coordinates with the uranyl centre but the CB[6] host just hangs on the alkyl chain like a bead. Since the pseudorotaxane linker has kept the molecular configuration of the pseudorotaxane precursor, the whole building unit is still in *trans*-mode. In term of the connecting pattern, mode 2 is similar to mode 1 and can be observed in **URCP4** and **URCP5** (Figure S11b). However, the building unit adopts a *cis*-mode conformation. It's not hard to imagine that

C7BPCA3@CB[6] tends to undergo a conformational flip and then coordinates with the uranyl centre (Figure 8b). Actually, such a conformational flip of the pseudorotaxane ligand is very rare in previously-reported uranyl coordination polyrotaxanes. In this case, it can be attributed to the weak binding between the host and guest components, which can endow the whole molecule much more flexibility. Mode 3 can only be observed in **URCP5** (Figure S11c), in which both the host and guest components of one pseudorotaxane ligand have synergistically coordinated with the same uranyl centre. As shown in Figure 8c, it seems that the **C7BPCA3**@CB[6] prefers to take a conformational flip like the supramolecular ligand in mode 2, following by coordinating with the uranyl centres through the carboxylate groups of **C7BPCA3**. Additionally, the special molecular conformation can provide the possibility for the CB[6] macrocycle surround **C7BPCA3** to chelate with the metal cation. This kind of synergetic coordination behavior of pseudorotaxane ligand can be attributed to the proximity effect existing between the carboxylate groups of **C7BPCA3** guest and the portal carbonyl groups of CB[6] host (Figure S12a). Relatively, for **C7BPCA4**@CB[6] with the functional carboxylate groups located at the *para*-positions[28], although the weakly binding could offer CB[6] the ability to coordinate with uranyl cations, the host and guest components tended to bond with different uranyl centre as no proximity effective could be observed (Figure S12b).

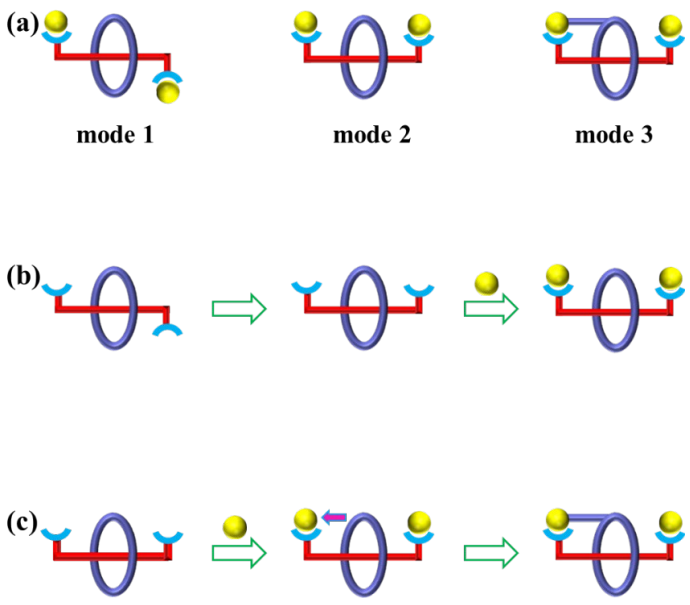

Figure 8. (a) Three coordination modes observed in **URCP1-URCP5**. (b) Diagram of mode 2 in **URCP4** and **URCP5**. (c) Diagram of mode 3 in **URCP5**.

This kind of proximity effects were also observed in our previous work involving a well-bonded pseudorotaxane ligand **C6BPCA3**@CB[6][31], in which the guest was hexyl-bridged. In that case, the proximity effect produced by the special molecular conformation of the supramolecular ligand, *i.e.*, *meta*-substituted carboxylate groups can effectively shorten the distance between the uranyl centers and the CB[6] host, giving the carbonyl groups on both portals the chance to chelate with the metal cations together with adjacent carboxylate groups of the **C6BPCA3** guest (Figure S12c). However, the guest length (d = 9.804 Å) of **C7BPCA3**@CB[6] is obviously longer than that of the **C6BPCA3**@CB[6] (d = 8.794 Å). This means that prolonging of the guest length may partially diminish the proximity effect given by the *meta*-substituted functional groups. As a consequence, CB[6] can only unilaterally coordinate with the uranyl center through portal carbonyl groups at one end but not both (Figure S12c).

FTIR, PXRD, TGA, and PL Analyses. A sufficient amount of crystal samples of **URCP1**–**URCP5** were collected and dried at 80 ºC overnight, which were carried out for FTIR analyses. As shown in Figure S13, the wide band around 3500 cm^{-1} should be attributed to the water molecules coordinated with the uranyl centres or those located in the crystal lattices. The pyridinium ring of **C7BPCA3**@CB[6] have shown their characteristic peaks at ~3080 cm^{-1}. The peaks in the range of 2900 ~ 3000 cm^{-1} should be assigned to the methylene and methine groups of **C7BPCA3** and CB[6]. The vibrations of the carboxylate groups of **C7BPCA3** and the carbonyl groups of CB[6] are observed in the range of 1570 ~ 1720 cm^{-1}. The existence of uranyl cation has been proven by the U=O stretching vibrations appearing in the region of 960 ~ 970 cm^{-1}. The peak at ~1470 belonging to C-N bond can also prove the existence of pyridinium, while those around 1370, 1320, 1270 and 1230 cm^{-1} come from the vibration of N-CO-N groups in CB[6]. The existence of uranyl cation for all coordination polymers has been proven by the U=O stretching vibrations appearing in the region of 960 ~ 970 cm^{-1}. Other peaks in fingerprint region have also indicated the existence of pyridinium ring of the pseudorotaxane ligand.

For PXRD, only **URCP1**, **URCP4** and **URCP5** show high phase purity, which is demonstrated by the good match between the experimental and simulated patterns of these compounds (Figure S14). For **URCP1**, all peaks in the experimental pattern are sharper than that in the simulated pattern, which might be caused by the loss of crystal water molecules during the drying process. For **URCP4**

and **URCP5**, the experimental patterns present some broadenings when compared with the simulated ones, especially those at higher 2θ. This may be caused by the size effect, as the grinding before carrying out PXRD may give much smaller crystals, although they might be obtained in micrometer-scale. The TGA results suggest that these three compounds have good thermal stability, and no obvious weight loss occurs below 350 ºC (Figure S15), except those of the crystal water molecules. When the temperature further increases, all compounds began to decompose, which might be due to the destruction of the pseudorotaxane linker and the breaking of the coordination bonds between the uranyl centers and supramolecular ligands.

Shown in Figure 9 are the PL spectra of **URCP1**, **URCP4** and **URCP5** with $UO_2(NO_3)_2·6H_2O$ acting as control. The difference of the luminescent features among these compounds are caused by their various coordination modes between the uranyl centers and the pseudorotaxane ligands.[40-41] The fluorescent peaks of **URCP1** are obviously broadened when compared with that of uranyl nitrate. This is due to that **URCP1** contains a dimeric uranyl centre, and the two crystallographically non-equivalent uranium atoms will interplay with each other in the luminescent emission. For **URCP4** and **URCP5**, the broadening of the PL spectra appears to be more obvious, which should also be explained by the overlap among different uranyl cations in multimeric centers. Red shifts can be observed for all the three compounds, which may be caused by the coordination of uranyl with the organic linker.

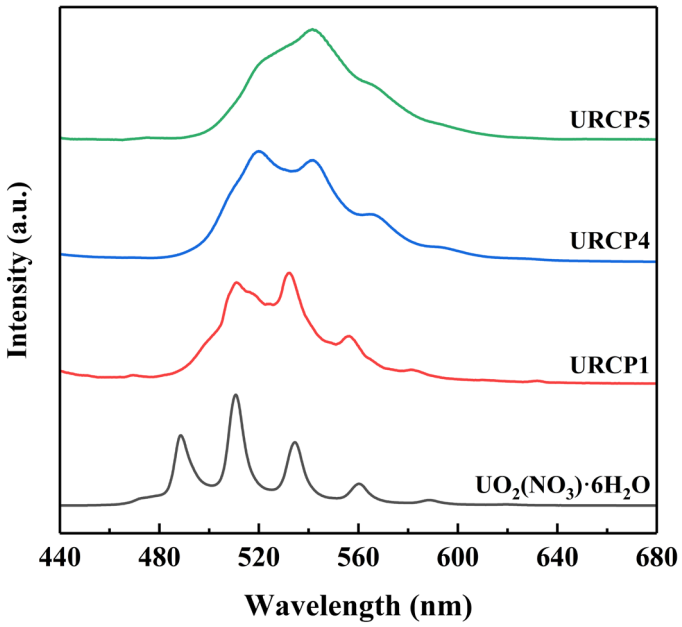

Figure 9. PL spectra of **URCP1**, **URCP4** and **URCP5** with uranyl nitrate as a comparison.

Conclusion

In this work, we proposed to introduce *meta*-substituted functional groups into weakly-bonded pseudorotaxane ligand, with an attempt to explore the proximity effect on uranyl coordination of weak-bonded CB[6]-bipyridinium pseudorotaxane ligands and achieve structure regulation of uranyl coordination polyrotaxanes. The strategy has been demonstrated to be effective, and five different URCPs varying from 1D to 2D have been obtained. Single crystal structure analyses show that the designed pseudorotaxane can exhibit rich conformational variety, and result in three metal coordination modes in the prepared URCPs. More interestingly, synergetic host-guest coordination is also observed in these uranyl coordination polyrotaxanes, which is totally different from the mode of its *para*-substituted pseudorotaxane analogue. It indicates that the impact of proximity effect on uranyl coordination can also be achieved in weak-bonded CB[6]-bipyridinium pseudorotaxane linkers. The outcome of this work can not only enrich the library of actinide-rotaxane coordination polymers, but can also provide some important hints for the design and synthesis of other metal-organic frameworks.

Conflicts of interest

The authors declare no competing financial interest.

Acknowledgment

This work is financially supported by the National Natural Science Foundation of China (21876122, 22076186, and 22076187). The National Science Fund for Distinguished Young Scholars (21925603) is also acknowledged. The authors also would like to thank Dr Meng Yang in College of Chemistry, Sichuan University, for his helpful assistance with X-ray single crystal measurements, solutions and refinements.

References

1. Dolgopolova, E. A.; Rice, A. M.; Shustova, N. B., Actinide-based MOFs: a middle ground in solution and solid-state structural motifs. *Chem Commun* **2018,** *54*, 6472-6483.

2. Martin, C. R.; Leith, G. A.; Shustova, N. B., Beyond structural motifs: the frontier of actinide-containing metal-organic frameworks. *Chem Sci* **2021,** *12*, 7214-7230.

3. Andrews, M. B.; Cahill, C. L., Uranyl bearing hybrid materials: synthesis, speciation, and solid-state structures. *Chem Rev* **2013,** *113*, 1121-1136.
4. Loiseau, T.; Mihalcea, I.; Henry, N.; Volkringer, C., The crystal chemistry of uranium carboxylates. *Coordin Chem Rev* **2014,** *266*, 69-109.
5. Wang, Y.; Liu, Z.; Li, Y.; Bai, Z.; Liu, W.; Wang, Y.; Xu, X.; Xiao, C.; Sheng, D.; Diwu, J.; Su, J.; Chai, Z.; Albrecht-Schmitt, T. E.; Wang, S., Umbellate distortions of the uranyl coordination environment result in a stable and porous polycatenated framework that can effectively remove cesium from aqueous solutions. *J Am Chem Soc* **2015,** *137*, 6144-7.
6. Hu, F. L.; Di, Z. Y.; Lin, P.; Huang, P.; Wu, M. Y.; Jiang, F. L.; Hong, M. C., An anionic uranium-based metal–organic framework with ultralarge nanocages for selective dye adsorption. *Cryst. Growth Des.* **2018,** *18*, 576-580.
7. Wang, Y.; Li, Y.; Bai, Z.; Xiao, C.; Liu, Z.; Liu, W.; Chen, L.; He, W.; Diwu, J.; Chai, Z.; Albrecht-Schmitt, T. E.; Wang, S., Design and synthesis of a chiral uranium-based microporous metal organic framework with high SHG efficiency and sequestration potential for low-valent actinides. *Dalton Trans* **2015,** *44*, 18810-18814.
8. Liu, C.; Wang, C.; Sun, Z. M., Conformational 2-fold interpenetrated uranyl supramolecular isomers based on (6,3) sheet topology: structure, luminescence, and ion exchange. *Inorg Chem* **2018,** *57*, 15370-15378.
9. Ai, J.; Chen, F. Y.; Gao, C. Y.; Tian, H. R.; Pan, Q. J.; Sun, Z. M., Porous anionic uranyl-organic networks for highly efficient Cs^+ adsorption and investigation of the mechanism. *Inorg Chem* **2018,** *57*, 4419-4426.
10. Xie, J.; Wang, Y.; Liu, W.; Yin, X.; Chen, L.; Zou, Y.; Diwu, J.; Chai, Z.; Albrecht-Schmitt, T. E.; Liu, G.; Wang, S., Highly sensitive detection of ionizing radiations by a photoluminescent uranyl organic framework. *Angew Chem, Int Ed* **2017,** *56*, 7500-7504.
11. Wang, Y.; Yin, X.; Liu, W.; Xie, J.; Chen, J.; Silver, M. A.; Sheng, D.; Chen, L.; Diwu, J.; Liu, N.; Chai, Z.; Albrecht-Schmitt, T. E.; Wang, S., Emergence of uranium as a distinct metal center for building intrinsic X-ray scintillators. *Angew Chem, Int Ed* **2018,** *57*, 7883-7887.
12. Liu, W.; Xie, J.; Zhang, L.; Silver, M. A.; Wang, S., A hydrolytically stable uranyl organic framework for highly sensitive and selective detection of Fe^{3+} in aqueous media. *Dalton Trans* **2018,** *47*, 649-653.
13. Hu, K. Q.; Wu, Q. Y.; Mei, L.; Zhang, X. L.; Ma, L.; Song, G.; Chen, D. Y.; Wang, Y. T.; Chai, Z. F.; Shi, W. Q., Novel viologen derivative based uranyl coordination polymers featuring photochromic behaviors. *Chem -Eur J* **2017,** *23*, 18074-18083.
14. Kong, X. H.; Hu, K. Q.; Mei, L.; Li, A.; Liu, K.; Zeng, L. W.; Wu, Q. Y.; Chai, Z. F.; Nie, C. M.; Shi, W. Q., Double-layer nitrogen-rich two-dimensional anionic uranyl-organic framework for cation dye capture and catalytic fixation of carbon dioxide. *Inorg Chem* **2021,** *60*, 11485-11495.
15. Andrew T. Kerr; Sayon A. Kumalah; K. T. Holman; Butcher, R. J.; Cahill, C. L., Uranyl coordination polymers incorporating η^5-cyclopentadienyliron-functionalized η^6-phthalate metalloligands: syntheses, structures and photophysical properties. *J Inorg Organomet Polym Mater* **2014,** *24*, 128-136.
16. Si, Z. X.; Xu, W.; Zheng, Y. Q., Synthesis, structure, luminescence and photocatalytic properties of an uranyl-2,5-pyridinedicarboxylate coordination polymer. *J Solid State Chem* **2016,** *239*, 139-144.
17. Vukotic, V. N.; Loeb, S. J., Coordination polymers containing rotaxane linkers. *Chem Soc Rev* **2012,** *41*, 5896-906.
18. Yang, X.; Giorgi, M.; Karoui, H.; Gigmes, D.; Hornebecq, V.; Ouari, O.; Kermagoret, A.; Bardelang, D., A single-crystal-to-single-crystal transformation affording photochromic 3D MORF crystals. *Chem Commun* **2019,** *55*, 13824-13827.
19. Wilson, B. H.; Abdulla, L. M.; Schurko, R. W.; Loeb, S. J., Translational dynamics of a non-degenerate molecular shuttle imbedded in a zirconium metal-organic framework. *Chem Sci* **2021,** *12*, 3944-3951.
20. Gholami, G.; Wilson, B. H.; Zhu, K.; O'Keefe, C. A.; Schurko, R. W.; Loeb, S. J., Exploring the dynamics of Zr-

based metal-organic frameworks containing mechanically interlocked molecular shuttles. *Faraday Discuss* **2021,** *225*, 358-370.

21. Li, F. Z.; Geng, J. s.; Hu, K. Q.; Zeng, L. W.; Wang, J. Y.; Kong, X. H.; Liu, N.; Chai, Z. F.; Mei, L.; Shi, W. Q., Temperature-triggered structural dynamics of non-coordinating guest moieties in a fluorescent actinide polyrotaxane framework. *Chem –Eur J* **2021,** *27*, 8730-8736.

22. Mei, L.; Shi, W. Q.; Chai, Z. F., Ordered entanglement in actinide-organic coordination polymers. *B Chem Soc Jpn* **2018,** *91*, 554-562.

23. Mei, L.; Wu, Q. Y.; Liu, C. M.; Zhao, Y. L.; Chai, Z. F.; Shi, W. Q., The first case of an actinide polyrotaxane incorporating cucurbituril: a unique 'dragon-like' twist induced by a specific coordination pattern of uranium. *Chem Commun* **2014,** *50* , 3612-3615.

24. Mei, L.; Xie, Z. N.; Hu, K. Q.; Wang, L.; Yuan, L. Y.; Li, Z. J.; Chai, Z. F.; Shi, W. Q., First three-dimensional actinide polyrotaxane framework mediated by windmill-like six-connected oligomeric uranyl: dual roles of the pseudorotaxane precursor. *Dalton Trans* **2016,** *45*, 13304-13307.

25. Mei, L.; Xie, Z. N.; Hu, K. Q.; Yuan, L. Y.; Gao, Z. Q.; Chai, Z. F.; Shi, W. Q., Supramolecular host–guest inclusion for distinguishing cucurbit[7]uril-based pseudorotaxanes from small-molecule ligands in coordination assembly with a uranyl center. *Chem -Eur J* **2017,** *23* 13995-14003.

26. Mei, L.; Wang, L.; Liu, C. M.; Zhao, Y. L.; Chai, Z. F.; Shi, W. Q., Tetranuclear uranyl polyrotaxanes: preferred selectivity toward uranyl tetramer for stabilizing a flexible polyrotaxane chain exhibiting weakened supramolecular inclusion. *Chem -Eur J* **2015,** *21*, 10226-10235.

27. Xie, Z. N.; Mei, L.; Hu, K. Q.; Xia, L. S.; Chai, Z. F.; Shi, W. Q., Mixed-ligand uranyl polyrotaxanes incorporating a sulfate/oxalate coligand: achieving structural diversity via pH-dependent competitive effect. *Inorg Chem* **2017,** *56*, 3227-3237.

28. Li, F. Z.; Mei, L.; Hu, K. Q.; Yu, J. P.; An, S. W.; Liu, K.; Chai, Z. F.; Liu, N.; Shi, W. Q., Releasing metal-coordination capacity of cucurbit[6]uril macrocycle in pseudorotaxane ligands for the construction of interwoven uranyl-rotaxane coordination polymers. *Inorg Chem* **2018,** *57*, 13513-13523.

29. Li, F. Z.; Mei, L.; Hu, K. Q.; An, S. W.; Wu, S.; Liu, N.; Chai, Z. F.; Shi, W. Q., Uranyl compounds involving a weakly bonded pseudorotaxane linker: combined effect of pH and competing ligands on uranyl coordination and speciation. *Inorg Chem* **2019,** *58*, 3271-3282.

30. Li, F. Z.; Mei, L.; An, S. W.; Hu, K. Q.; Chai, Z. F.; Liu, N.; Shi, W. Q., Kinked-helix actinide polyrotaxanes from weakly bound pseudorotaxane linkers with variable conformations. *Inorg Chem* **2020,** *59*, 4058-4067.

31. Li, F. Z.; Geng, J. S.; Hu, K. Q.; Yu, J. P.; Liu, N.; Chai, Z. F.; Mei, L.; Shi, W. Q., Proximity effect in uranyl coordination of the cucurbit[6]uril-bipyridinium pseudorotaxane ligand for promoting host-guest synergistic chelating. *Inorg Chem* **2021,** *60*, 10522-10534.

32. Sheldrick, G. M., A short history of SHELX. *Acta Crystallogr, Sect D: Struct Biol* **2008,** *64*, 112-122.

33. Usón, I.; Sheldrick, G. M., An introduction to experimental phasing of macromolecules illustrated by SHELX; new autotracing features. *Acta Crystallogr, Sect D: Struct Biol* **2018,** *74*, 106-116.

34. Dolomanov, O. V.; Bourhis, L. J.; Gildea, R. J.; Howard, J. A.; Puschmann, H., *OLEX2*: a complete structure solution, refinement and analysis program. *J Appl Crystallogr* **2009,** *42*, 339-341.

35. Spek, A. L., PLATON SQUEEZE: a tool for the calculation of the disordered solvent contribution to the calculated structure factors. *Acta Crystallogr, Sect C: Struct Chem* **2015,** *71*, 9-18.

36. Gao, R. H.; Huang, Y.; Chen, K.; Tao, Z., Cucurbit[*n*]uril/metal ion complex-based frameworks and their potential applications. *Coordin Chem Rev* **2021,** *437*, 213741.

37. Ni, X. L.; Xiao. X.; Cong H.; Liang L. L.; Cheng K.; Cheng X. J.; Ji N. N.; Zhu Q. J., Xue S. F. and Tao Z, Cucurbit[*n*]uril-based coordination chemistry_ from simple coordination complexes to novel poly-dimensional

coordination polymers. *Chem Soc Rev* **2013,** *42*, 9480-9508.
38. Huang, Y.; Gao, R. H.; Liu, M.; Chen, L. X.; Ni, X. L.; Xiao, X.; Cong, H.; Zhu, Q. J.; Chen, K.; Tao, Z., Cucurbit[n]uril-based supramolecular frameworks assembled through outer-surface interactions. *Angew Chem, Int Ed* **2021,** *60*, 15166-15191.
39. Thuery, P., Uranyl ion complexes with cucurbit[*n*]urils (*n* = 6, 7, and 8): A new family of uranyl-organic frameworks. *Cryst Growth & Des* **2008,** *8*, 4132-4143.
40. Thuéry, P.; Harrowfield, J., Structural variations in the uranyl/4,4'-biphenyldicarboxylate system. rare examples of 2D→3D polycatenated uranyl-organic networks. *Inorg Chem* **2015,** *54*, 8093-8102.
41. A.F. Leung; L. Hayashibara; Spadar, J., Fluorescence properties of uranyl nitrates. *J Phys Chem Solids* **1999,** *60*, 299-304.

Table of contents entry

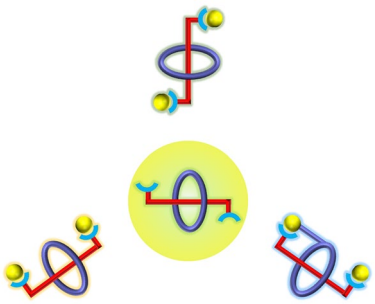

The proximity effect of weakly-bonded CB[6]-bipyridinium pseudorotaxane has great impact on the coordination mode of related uranyl polyrotaxane. Three different coordination modes have appeared, resulting in structure variety in the prepared uranyl compounds.